Measurement of the Expansion of Picosecond Laser-Produced Plasmas Using Resonance Absorption Profile Spectroscopy

O. L. Landen, D. G. Stearns, and E. M. Campbell
Lawrence Livermore National Laboratory, University of California, P.O. Box 808 Livermore, California 94550
(Received 18 May 1989)

Time-resolved submicron density scale lengths in picosecond laser-produced plasmas are measured using resonance absorption profile spectroscopy. The density scale length at critical density is inferred from the angle and polarization dependence of the absorption of a picosecond laser pulse in a preformed plasma. The early expansion of picosecond laser-produced plasmas produced from a Au target is studied, with measured scale lengths in the range of ~1000–5000 Å.

PACS numbers: 52.40.Nk, 52.50.Jm, 52.70.La

The interaction of high-intensity picosecond and subpicosecond laser pulses with solid targets is an area of both fundamental and practical current interest.[1-4] For sufficiently high absorbed laser fluence (>0.1 J/cm^2), an incident ("pump") pulse creates a high-density plasma which rapidly expands to form a density gradient between the solid target and vacuum. In this Letter we report the first measurements of the initial stages of hydrodynamic expansion in such ultrashort-scale-length plasmas.

We have used resonance absorption profile spectroscopy to measure the plasma density scale length at critical density with, for the first time, submicron accuracy and picosecond temporal resolution. The technique consists of indirectly measuring the resonance absorption[5] by the preformed plasma of a second picosecond laser pulse (the "probe" pulse). The characteristic dependence of resonance absorption on the angle of incidence and polarization of the probe laser pulse is used to unambiguously determine the density scale length. The temporal evolution of the scale length is measured with picosecond accuracy by varying the time delay between the pump and probe pulses. We note that resonance absorption has been used before to infer plasma density scale lengths.[3,4,6] In each case, however, a single laser pulse (sometimes including a prepulse[3,4]) was used to both create and simultaneously interact with the plasma, leading to difficulties in the interpretation of the results. The important distinction and advantage of the present technique is that the pump-probe configuration allows the initial formation of the plasma and the measurement of the scale length to be decoupled.

The absorption of the probe pulse has been modeled for arbitrary scale length L and incident angle θ by numerically integrating the Helmholtz wave equations[7] for both P- and S-polarized probe beams. The usual plasma dielectric function was used, $\epsilon = 1 - \omega_p^2/\omega(\omega + i\nu)$, where ω and $\omega_p = (4\pi n_e e^2/m)^{1/2}$ are the laser and local plasma frequency, respectively, n_e is the electron density, and ν is the phenomenological damping coefficient. For the plasmas studied in this experiment ($T_e < 200$ eV) the dominant damping mechanism is assumed to be electron-ion collisions. Landau damping of resonantly excited plasma waves can be neglected when the electron mean free path, λ_{mfp}, is much less than the density scale length, a condition always satisfied in these plasmas.[8] Other absorption mechanisms such as laser-driven parametric instabilities,[9] $J \times B$ heating,[10] irreversible electron acceleration,[11] and multiphoton ionization,[12] which become important at high laser intensities ($I\lambda^2 > 10^{14}$ W cm^{-2} μm^2) and/or long scale lengths ($kL \gg 10$, where $k = \omega/c$ is the laser wave number), could be ignored under our experimental conditions. Furthermore, the experimental probe-light pressure and associated electron quiver energy (3.2 eV at 10^{14} W/cm^2) were generally kept small compared to the plasma pressure and electron temperature,[13] permitting the use of linearized wave equations and the field-independent dielectric function. We assumed an exponential density profile, $n_g \propto e^{z/L}$, consistent with a one-dimensional model for isothermal plasma expansion,[14] and a density-dependent collision frequency $\nu \propto n_e$.[15]

Computational results are shown in Fig. 1(a). The difference of the absorption of P- and S-polarized light is plotted as a function of angle of incidence (with respect to target normal) for various critical density scale lengths, $kL = 0$–10, and for a collisionality of $\nu_c/\omega = 0.1$, where ν_c is the collision frequency at the critical density. In the limit $kL \to 0$ the curves reduce to the well-known solution of the Fresnel equations for an abrupt interface. For $kL > 0.1$, the curves show the characteristic Ginzburg profile associated with resonance absorption.[5] In particular, in the limit of $kL \gg 1$ and $\nu_c/\omega \ll 1$, the numerical results tend towards an analytic solution for the resonance absorption, $A(\theta)$, of P-polarized light in an exponential density profile,

$$A(\theta) \propto (kL)^{2/3} \sin^2\theta e^{-4kL(\sin\theta - \theta\cos\theta)}.$$

For finite ν_c and increasing kL, the amount of resonance absorption decreases [see Fig. 1(a)] because of increas-

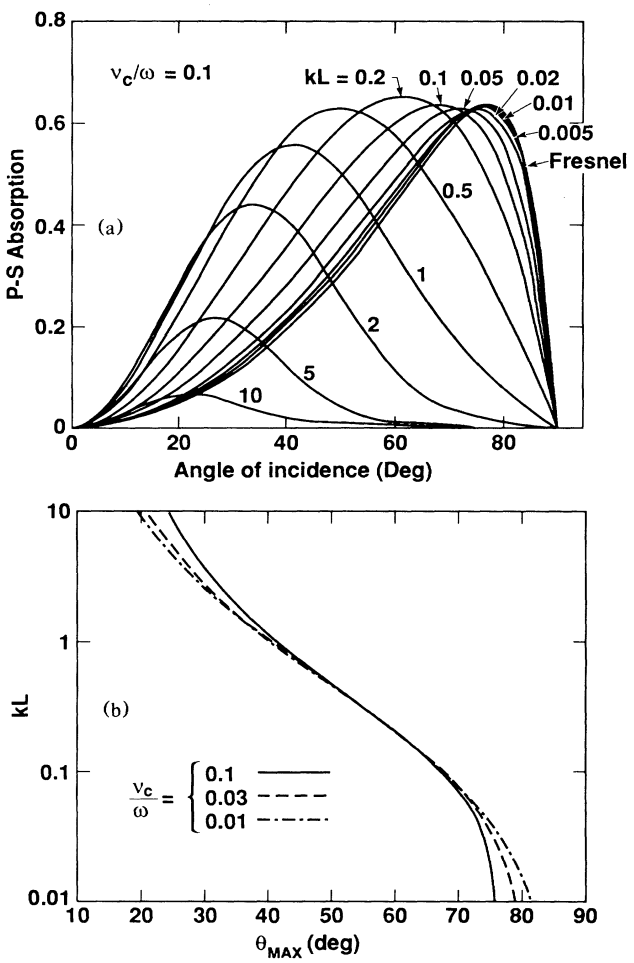

FIG. 1. (a) Calculated difference in absorption of *P*- and *S*-polarized light as a function of angle of incidence for different values of the (dimensionless) density scale length kL. (b) The angle, θ_{max}, of the maximum difference in the absorption of *P*- and *S*-polarized light as a function of density scale length kL for three different values of the damping parameter ν_c/ω.

ing beam depletion in the expanding corona via inverse bremsstrahlung. The absorption profiles are found to be only weakly dependent on the collision frequency ν_c for $(\nu_c/\omega)kL \ll 1$, and are strongly dependent on scale length L for $0.05 < kL < 5$. This is illustrated explicitly in Fig. 1(b), where we plot kL as a function of the angle of maximum absorption, θ_{max}, for three values of ν_c/ω. It is evident that the measurement of θ_{max} provides an accurate determination of scale lengths between 50 and 5000 Å (assuming $\lambda \sim 6000$ Å), independent of the exact value of the plasma collision frequency.

The laser consisted of an amplified synchronously pumped 3.5-mJ, 1-ps dye laser operating at 583 nm and at a repetition rate of 1.25 Hz.[16] Care was taken to keep the prepulse energy fluence on target below 0.1 J/cm^2, the damage threshold for subnanosecond pulses,[17] to avoid production of a long-scale-length plasma before the arrival of the main picosecond pulse.[3] Following the main pulse by ~ 7 ps was a postpulse of ~ 5 ps duration containing typically $\sim 10\%$ of the total energy. The beam was split to provide optically synchronized pump and probe pulses. The pump pulse, *S* polarized, was sent through a variable delay line and focused by an $f/20$ lens to a 70–130-μm-diam spot on the target. The probe pulse, either *S* or *P* polarized, was focused by an $f/10$ lens to a 25-μm-diam spot centered on the larger focal spot defined by the pump pulse. The relative delay between the pulses was calibrated to 1 ps accuracy using a noncollinear type-II cross correlation in a 1-mm-thick β-$BaBO_4$ crystal.

The target consisted of a 3-in.-diam polished silicon wafer (3 Å rms surface roughness) overcoated with ~ 5000 Å of gold. The target was mounted on remotely driven translation and rotation stages so that the laser could fire on a fresh target surface and at a different angle of incidence on each shot. The pump pulse was oriented so that its angle of incidence varied only between $\pm 35°$, thereby keeping the energy density on target constant to within 20%.

The absorption of the probe pulse in the preformed plasma was measured indirectly by monitoring the soft-x-ray yield in an energy band of 300–1500 eV. The x-ray signal due to the pump pulse was generally less than 20% of the total yield, and could be measured independently and subtracted out when necessary. The time-integrated soft-x-ray emission was detected using a Channeltron detector filtered with a 0.5-μm-Al/0.3-μm-Lexan foil. The Channeltron was positioned at a viewing angle of 60° (with respect to the target normal) and rotated with the target. Both the x-ray signal and a monitor signal of the incident laser energy were recorded on each shot. An angular profile was collected by rotating the target through 0°–70° during the course of 160 laser shots.

The soft-x-ray yield, $Y(\theta)$, was measured in each case for both *S*- and *P*-polarized probe pulses. An example of raw data is shown in Fig. 2, where the difference in the x-ray yield obtained using *S*- and *P*-polarized light is plotted as a function of incident angle at several different time delays. The pump and probe irradiances in this case were 2×10^{13} and 1×10^{14} W/cm^2, respectively. Note that the angular position of the peak in the x-ray yield in Fig. 2 decreases with increasing time delay, consistent with an increasing scale length in an expanding plasma [see Fig. 1(a)]. For a delay of 200 ps we observed that the absorption profiles for *S*- and *P*-polarized light were essentially identical. We attribute this to a suppression of resonance absorption as the scale length becomes long enough to absorb the probe pulse before it reaches critical density. It is also possible that rippling of the critical-density surface upon expansion, induced by inhomogeneities in the pump pulse, results in a loss of

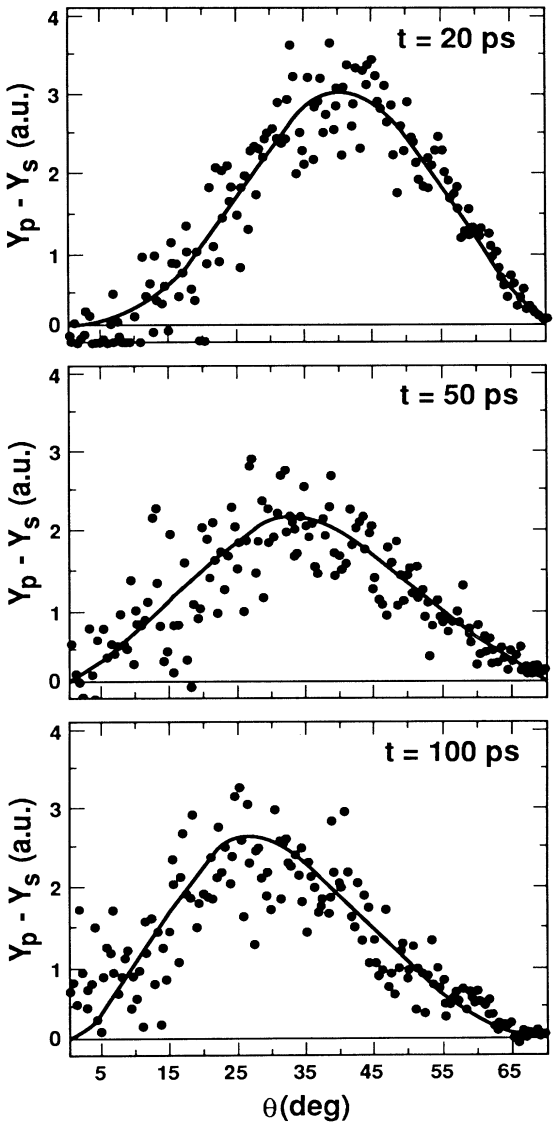

FIG. 2. Difference in the x-ray yields produced by *P*- and *S*-polarized probe pulses as a function of the angle of incidence. Data are shown for time delays between the pump and probe pulses of 20, 50, and 100 ps. The pump and probe irradiances were 2×10^{13} and 1×10^{14} W/cm^2, respectively. The curves fitted to the data points are provided as a visual aid to the reader.

distinction between *S* and *P* polarization.[18]

At probe-pulse intensities greater than 2×10^{14} W/cm^2 it was found that the angular profiles of the x-ray yield varied with intensity, implying that the probe pulse was perturbing the preformed plasma on the time scale of the measurement (1 ps). In particular, the position of the peak yield moved to larger angles, indicative of a reduced scale length. We attribute the profile steepening to a density-dependent ionization rate. At higher probe intensities, when the heating rate can exceed the ionization rate, the plasma is unable to maintain an equilibrium ionization balance during the picosecond pulse. Under such nonequilibrium conditions, the larger ionization rate at the higher densities results in a steepened profile. Hence to accurately measure the scale length of the preformed plasma it was necessary to limit the probe-pulse intensity to $\leq 1\times10^{14}$ W/cm^2.

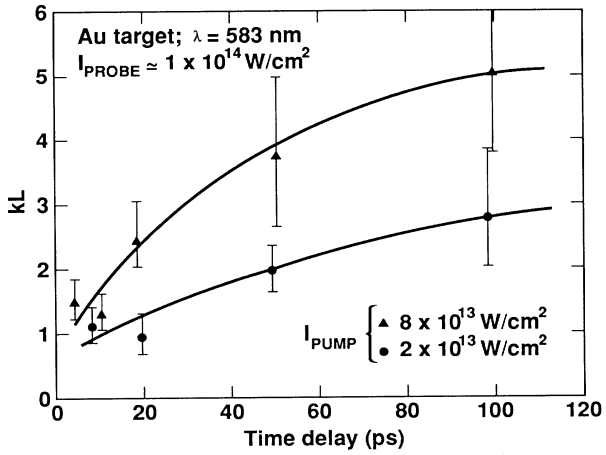

FIG. 3. Variation of the density scale length *kL* during the first 100 ps, measured at two different values of pump irradiance. The curves are provided as a visual aid to the reader.

The scale length of the preformed plasma was determined by comparing the position of the peak in the x-ray yield to the theoretical maxima in absorption [Fig. 1(b)], adjusted to account for the nonlinear relationship between absorption and x-ray yield, and for the variation in the focal area with incident angle.[19] A value of $\nu_c/\omega = 0.1$ was used throughout the analysis. This value was determined self-consistently from measurements of the specular reflectivity in conjunction with the implicit scale lengths, and is comparable to the values quoted in Ref. 2 for similar plasma conditions. Moreover, we note that in the range $0.05 > kL > 5$, the determination of the scale length is relatively insensitive to the choice of ν_c [see Fig. 1(b)].

The temporal evolution of the scale length of the preformed plasma at critical density is plotted in Fig. 3 for two pump irradiances of 2×10^{13} and 8×10^{13} W/cm^2. As expected, the plasma produced at the higher irradiance expands more rapidly. In both cases, the expansion velocity is observed to decrease with time as the plasma cools. Analytical models for the expansion can be derived assuming either isothermal or adiabatic conditions. The isothermal description seems more physically plausible because (1) thermal conduction in the plasma is sufficiently rapid to suppress large temperature gradients, and (2) heat conduction into the cold dense plasma above critical density can be significant on the picosecond time scale.[3] For one-dimensional isothermal expansion, the expansion velocity of the critical-density surface is given by[14] $c_s \equiv dL/dt = (ZT_e/m_i)^{1/2}$, where Z is the average charge state of the plasma and m_i is the

ion mass. The observed expansion velocities vary from 2×10^6 cm/s (ZT_e = 800 eV) at 10 ps to $\sim10^5$ cm/s ($ZT_e\sim2$ eV) at 100 ps. Calculated values[3] for electron cooling rates, three-body recombination rates, and thermalization rates with ions in these picosecond plasmas ($\geq 10^{11}$ s^{-1}) are consistent with the rapid decrease in ZT_e and the observed deceleration of the critical-density surface. A detailed comparison of these experimental results to computer modeling of the hydrodynamic expansion will be presented in a future publication.

In summary, resonance absorption profile spectroscopy has been used to infer submicron density scale lengths in laser-produced plasmas with picosecond time resolution. The technique is most sensitive for measuring density scale lengths in the range of $0.05 < kL < 5$, which represents greater than an order-of-magnitude improvement in resolution over interferometric techniques.[20] As a demonstration of the technique, the hydrodynamic evolution of a cooling and recombining picosecond laser plasma has been measured for the first time.

This work was performed under the auspices of the U.S. Department of Energy by Lawrence Livermore National Laboratory under Contract No. W-7405-Eng-48.

[1]M. M. Murnane, H. C. Kapteyn, and R. W. Falcone, Phys. Rev. Lett. **62**, 155 (1989); D. Kühlke, U. Herpers, and D. von der Linde, Appl. Phys. Lett. **50**, 1785 (1987); O. L. Landen, E. M. Campbell, and M. D. Perry, Opt. Commun. **63**, 253 (1987); C. H. Nam *et al.*, Phys. Rev. Lett. **59**, 2427 (1987); O. R. Wood, II, *et al.*, Appl. Phys. Lett. **53**, 654 (1988); G. Kühnle *et al.*, Appl. Phys. B **47**, 361 (1988); J. A. Cobble *et al.*, Phys. Rev. A **39**, 454 (1989).

[2]H. M. Milchberg *et al.*, Phys. Rev. Lett. **61**, 2364 (1988).

[3]D. G. Stearns *et al.*, Phys. Rev. A **37**, 1684 (1988).

[4]J. C. Kieffer *et al.*, Phys. Rev. Lett. **62**, 760 (1989).

[5]V. L. Ginzburg, *The Propagation of EM Waves in Plasmas* (Pergamon, New York, 1970), p. 260.

[6]R. Dinger, K. Rohr, and W. Weber, Laser Part. Beams **5**, 691 (1987); J. E. Balmer and R. P. Donaldson, Phys. Rev. Lett. **39**, 1084 (1977); A. G. M. Maaswinkel, K. Eidmann, and R. Sigel, Phys. Rev. Lett. **42**, 1625 (1979); B. Luther-Davies, Opt. Commun. **37**, 197 (1981).

[7]D. W. Phillion *et al.*, Phys. Fluids **20**, 1892 (1977).

[8]The condition $\lambda_{mfp}\ll L$ was always satisfied by the plasmas studied in this experiment, where $L > 1000$ Å and $\lambda_{mfp} < 30$ Å for $T_e < 200$ eV.

[9]W. L. Kruer and K. Estabrook, Phys. Fluids **28**, 430 (1985).

[10]F. Brunel, Phys. Rev. Lett. **59**, 52 (1987).

[11]R. B. White, C. S. Liu, and N. M. Rosenbluth, Phys. Rev. Lett. **31**, 520 (1973).

[12]M. D. Perry *et al.*, Phys. Rev. Lett. **60**, 1270 (1988).

[13]J. R. Albritton and A. B. Langdon, Phys. Rev. Lett. **45**, 1794 (1980).

[14]W. L. Kruer, *The Physics of Laser Plasma Interactions* (Addison-Wesley, Redwood City, 1988), p. 116.

[15]We implicitly assumed that the plasma temperature and average charge state are spatially invariant.

[16]M. D. Perry *et al.*, Opt. Lett. **14**, 42 (1989).

[17]P. B. Corkum *et al.*, Phys. Rev. Lett. **61**, 2886 (1988).

[18]J. J. Thomson *et al.*, Phys. Fluids **21**, 707 (1978).

[19]The dependence of the x-ray yield, Y, on absorbed probe energy, E, was found to obey a power law $Y\propto E^{\alpha}$. Values of the parameter α were determined for each time delay and were in the range 1–2. By including a geometric correction for the angular dependence of the focal area, the x-ray yield could be directly related to the absorption. A detailed description of the analysis will be presented in a future publication.

[20]A. Raven and O. Willi, Phys. Rev. Lett. **43**, 278 (1979); M. D. J. Burgess, R. Dragila, and B. Luther-Davies, Opt. Commun. **52**, 189 (1984); R. Fedosejevs *et al.*, Phys. Fluids **24**, 537 (1981).